Electronic Supplementary Material (ESI) for Materials Chemistry Frontiers.

Supporting Information

Lewis Acidity Adjustable Organic Ammonium Cation Derived Robust Protecting Shield for Stable Aqueous Zinc-ion Batteries by Inhibiting Tip Effect

Siyi Qian[a,+], Jinqiu Zhou[a,+], Mingji Peng[b], Yijun Qian[c,*], Yuan Meng[a], Yuzhuo Jiang[a], Xu Zeng[a], Jie Liu[a,*], Tao Qian[a,d*], Chenglin Yan[b,d]

[a] School of Chemistry and Chemical Engineering, Nantong University, Nantong 226019, China

[b] Soochow Institute for Energy and Materials Innovations, College of Energy, Key Laboratory of Advanced Carbon Materials and Wearable Energy Technologies of Jiangsu Province, Soochow University, Suzhou 215006, China

[c] Institute for Frontier Materials, Deakin University, Geelong, Victoria 3220, Australia

[d] Light Industry Institute of Electrochemical Power Sources, Suzhou 215006, China

[+] The two authors contribute equally to this work.

*E-mail: qiantao@ntu.edu.cn (T. Q).

*E-mail: jliu93@ntu.edu.cn (J. L).

*E-mail: qianyij@deakin.edu.au (Y. Q).

Experimental section

Materials

$ZnSO_4 \cdot 7H_2O$ (>99.0%), tetrabutylammonium chloride hydrate (≥98.0%) and tetramethylammonium chloride (≥98.0%) were purchased from Sigma-Aldrich Chemical Co. Tetraethylammonium chloride (>98.0%) was purchased from TCI Co. All reagents were used directly without further purification. All aqueous electrolytes used deionized water as the solvent.

Materials Characterizations

The in-situ optical microscope (Caikon DMM-330C) was employed to observe the growth of zinc dendrites in symmetric Zn//Zn batteries. SEM images were collected on the GeminiSEM 300 with an accelerating voltage of 5 kV and it was employed to observe the morphology of anode surface in Zn//Cu batteries after 20 cycles.

Battery Assembly

The Zn//Zn symmetrical battery which consists of two zinc sheets (Φ16 mm) and a glass fiber separator (Φ16 mm) with 100 μL electrolyte (2 M $ZnSO_4$ without/with 4 wt% additive) were sandwiched together in a CR2032 coin cell and crimped in the air. The Zn//Cu cell used for the CE test consists of a piece of Cu foil (Φ 12 mm), a Zn chip (Φ 16 mm) and a glass fiber separator (Φ 16 mm) with 100 μL electrolyte (2 M $ZnSO_4$ without/with 4 wt% additive). The cathode material which used in the full cell is a mixture of $LiMnO_2$ (LMO), super phosphorus and Teflon (dissolved in water) in a mass ratio of 7:2:1. The resulting mixture is cast onto a stainless steel mesh and pressed with a roller press at the pressure of 2.5 tons. And then the cathode material was dried at 80 ℃ for 12 hours in a vacuum oven. After drying, use a tablet press to cut them into 12 mm diameter pellets (each cathode pellet is loaded with ~1.5 mg cm–2 LMO). The Zn//LMO full-cell is the CR2032 coin cell composed of a LMO cathode pellet (Φ12 mm), a zinc sheet (Φ16 mm), a glass fiber separator (Φ16 mm) with 100 μL electrolyte (2 M $ZnSO_4$ and 1 M Li_2SO_4 without/with 4 wt% additive).

Electrochemical Tests

Galvanostatic charge-discharge cycling tests of Zn//LMO full cells and CE tests of Zn//Cu cells are performed on the Neware BTS4000 battery test instrument. In addition, the polarization of the Zn//Zn symmetrical cell under different conditions was also performed in this battery test instrument. Cyclic voltammetry (CV) measurements of Zn//$LiMnO_2$ full cells were carried out on an electrochemical workstation of CHI660E at 1 mV s^{-1}, and the voltage varied between 2.2 V and 1 V. The electrochemical

stability windows of the electrolytes without/with 4 wt% TEAC were tested by linear sweep voltammetry experiments at 1 mV s^{-1} with a typical three-electrode system, where platinum wire serves as working and counter electrodes, Ag/AgCl serves as reference electrode. Corresponding electrochemical impedance spectroscopy (EIS) studies also performed on the electrochemical workstation of CHI660E, and the frequency varied from 10^6 Hz to 10^{-3} Hz with an amplitude of 5 mV. The Tafel curves of Zn symmetric cells in different electrolytes were carried out on the workstation by the technique of Tafel Plot, and the voltage ranged from −1.04 V to −0.87 V.

DFT computational method

The Spin-polarized DFT calculation using the Vienna ab initio simulation package (VASP) was adopted to simulate ionic binding capacity including Zn^{2+}, TMA^+, TEA^+ and TBA^+ in the Zn-111 Surface. The Perdew–Burke–Ernzerhof with generalized gradient approximation (GGA) was adopted to describe the electron–electron interaction. An energy cutoff of 450 eV was used, and a k-point sampling set of 3 × 3 × 1 was tested to be converged. The criterion for all structural optimizations was set to 10^{-5} eV for electronic energy convergence and Hellmann−Feynman force less than 0.02 eV $Å^{-1}$ for ionic relaxation loop. The vacuum space along the z-direction is set to be 15 Å. To account for the strong on-site coulombic interaction of localized d electrons, the Hubbard-like term (U_{Zn} = 3.5 eV) was added into the DFT calculation. The van der Waals dispersion forces and solvation effects in aqueous solution were included using the zero damping DFT-D3 method of Grimme and Poisson-Boltzmann implicit solvation model as implemented in VASPSOL. The visualization for electronic and structural analysis (VESTA) was used to straightforwardly visualize the charge distribution of each model.

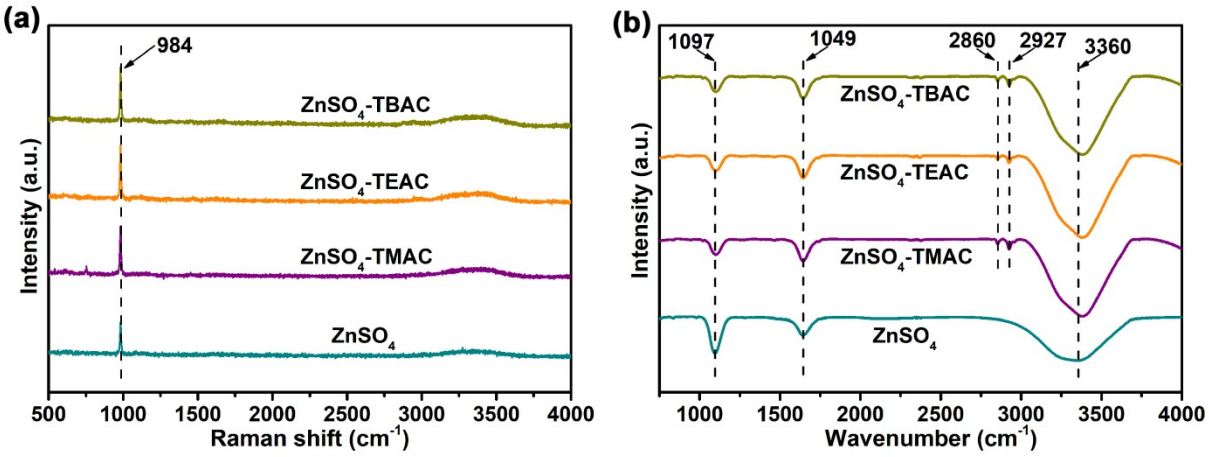

Figure S1. (a) Raman and (b) FTIR spectra of different electrolytes.

As shown in Fig. S1a, the symmetric stretching band (984 cm^{-1}) of SO_4^{2-} could be detected, and this could be also confirmed by FTIR spectrum of different electrolytes in Fig. S1b.[S1] The absorption peaks at 1049 cm^{-1} and 1097 cm^{-1} were attributed to the triply degenerate vibrations of SO_4^{2-}.[S2] New absorption peaks at 2860 $cm^{-1}$and 2927 cm^{-1} were introduced due to the addition of additives, which were dominated by strong C–H bond stretching vibrations of organic ammonium cations.[S3] Furthermore, the blue shift of the peak at 3360 cm^{-1} (O–H stretching) indicated that the addition of additives has changed the solvation structure, confirming the effect of added organic ammonium cations on the electrolytes.[S4]

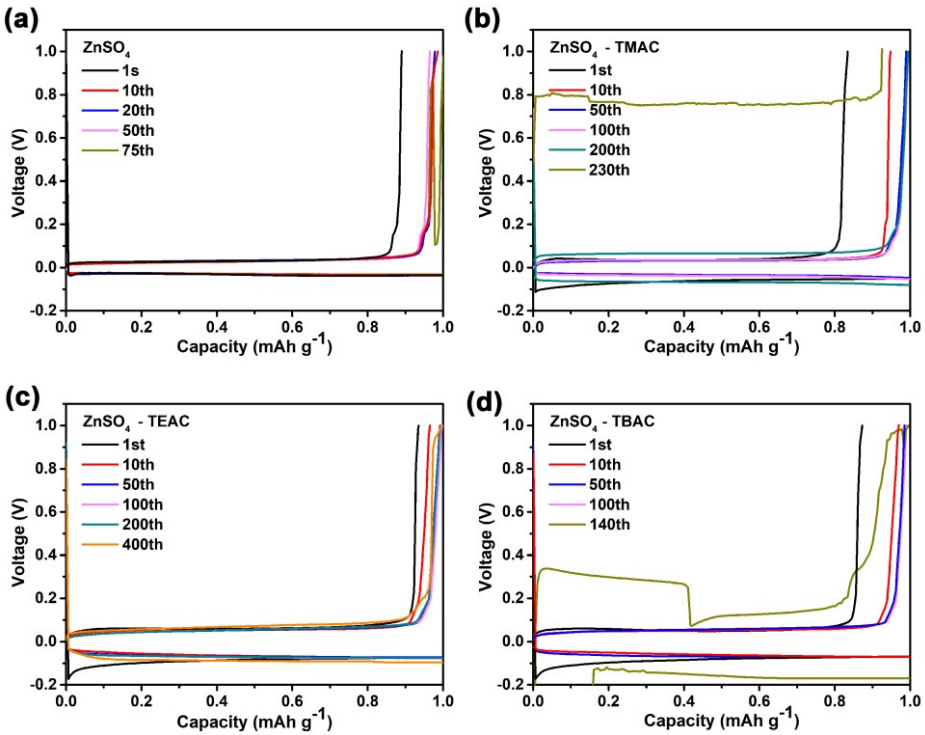

Figure S2. Charge/discharge curves of Zn//Cu cells in different electrolyte obtained from Fig. 2a.

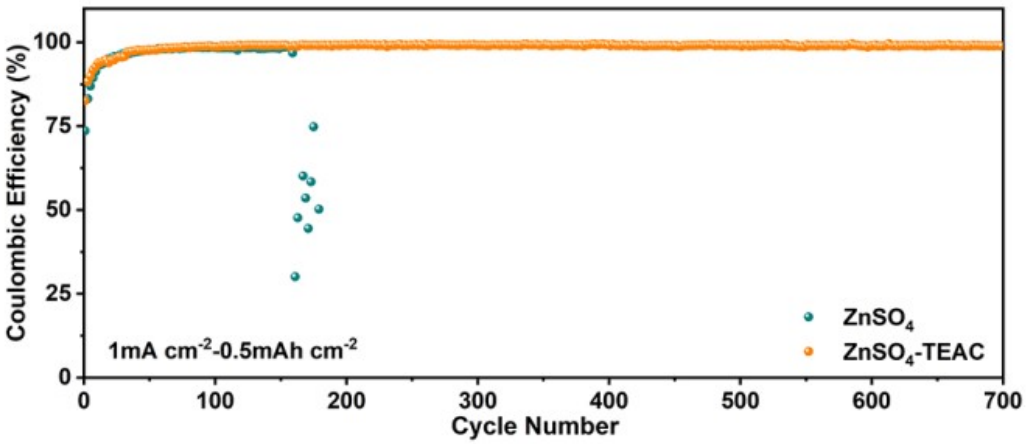

Figure S3. Coulombic efficiency of Zn//Cu coin cells with/without TEA^+ in the electrolytes at 1 mA cm^{-2} and 0.5 mAh cm^{-2}.

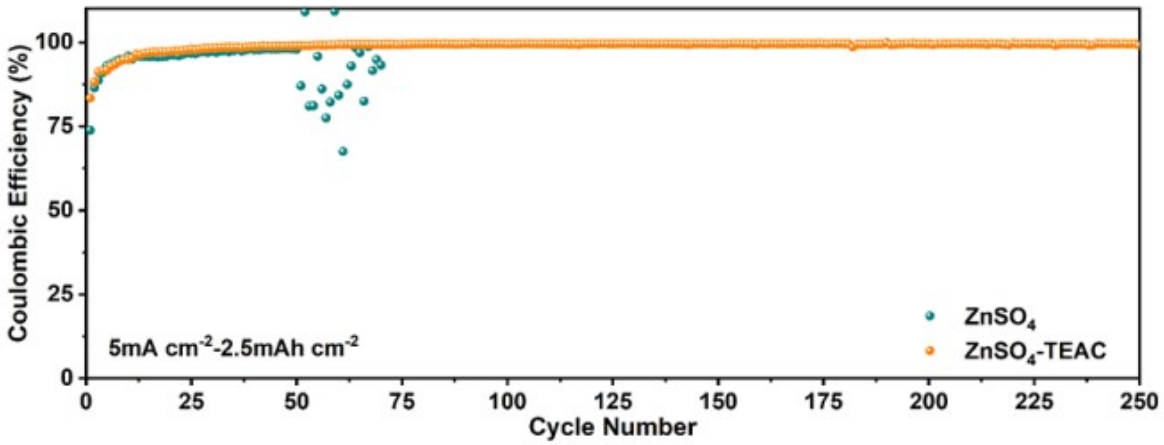

Figure S4. Coulombic efficiency of Zn//Cu coin cells with/without TEA^+ in the electrolytes at 5 mA cm^{-2} and 2.5 mAh cm^{-2}.

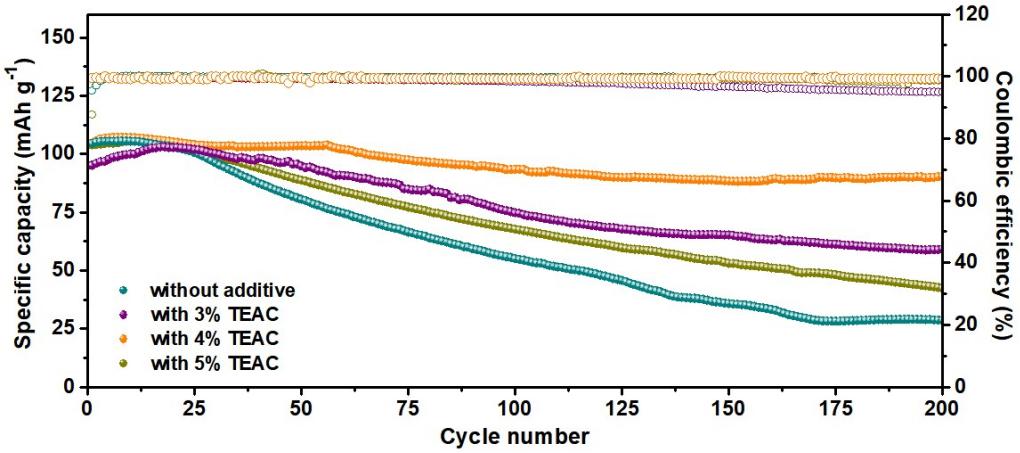

Figure S5. Cycling stability and efficiency of Zn//$LiMnO_2$ cells in electrolytes with different contents of TEAC additive at 2 C.

To explore the most suitable additive content, at the rate of 2 C, we tested the long-term cycling stability of Zn//$LiMnO_2$ batteries with different contents of TEAC additive in the electrolyte (Fig. S5). In the electrolyte with 4 wt% TEAC, the stability of Zn//$LiMnO_2$ battery was improved to the greatest extent.

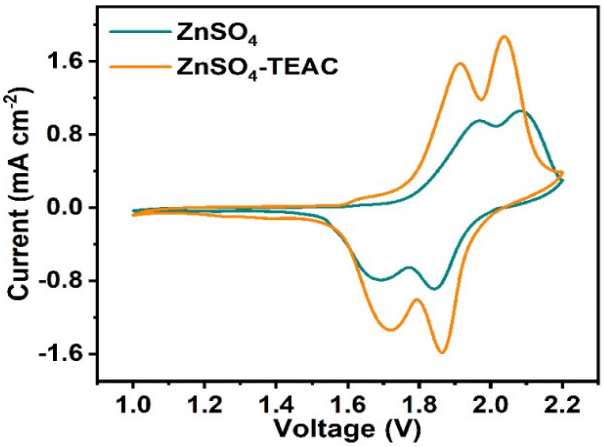

Figure S6. CV tests of Zn//$LiMnO_2$ full cells in the electrolyte without/with TEAC additive.

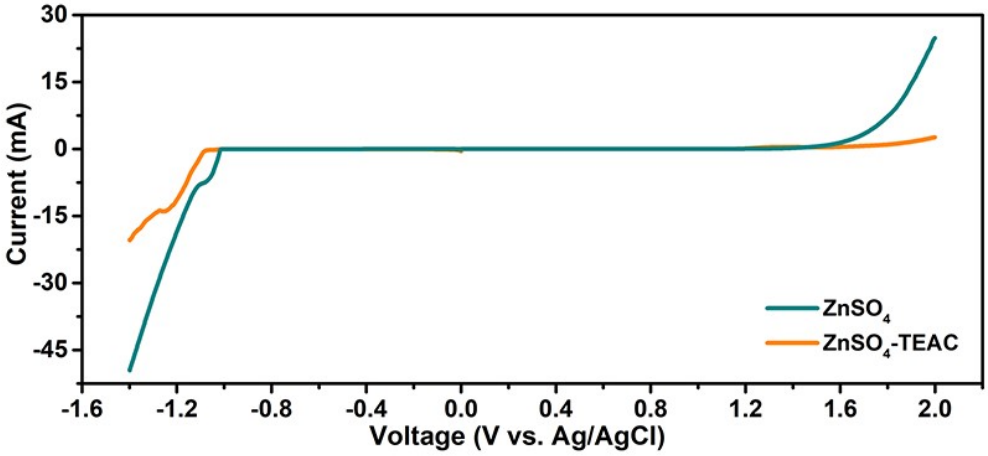

Figure S7. The electrochemical stability windows of the electrolyte without/with TEAC additive.

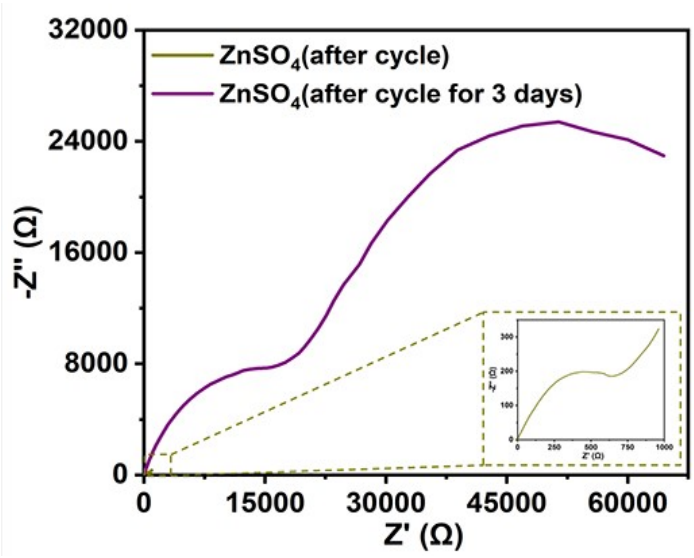

Figure S8. EIS curves of the Zn//Zn symmetric cell in the $ZnSO_4$ electrolyte after 20 cycles and after 20 cycles for 3 days.

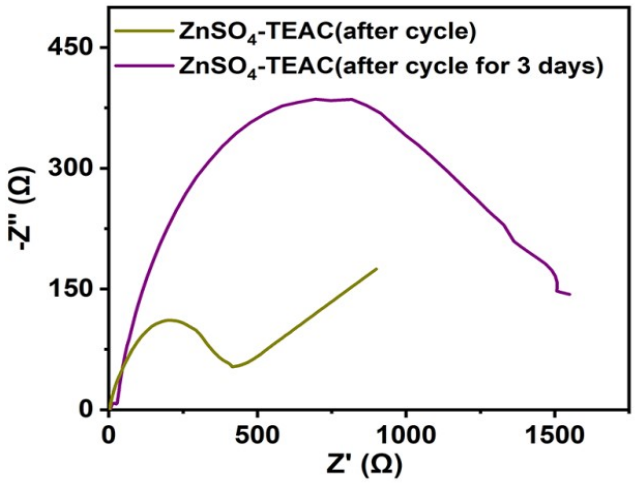

Figure S9. EIS curves of the Zn//Zn symmetric cell in the $ZnSO_4$-TEAC electrolyte after 20 cycles and after 20 cycles for 3 days.

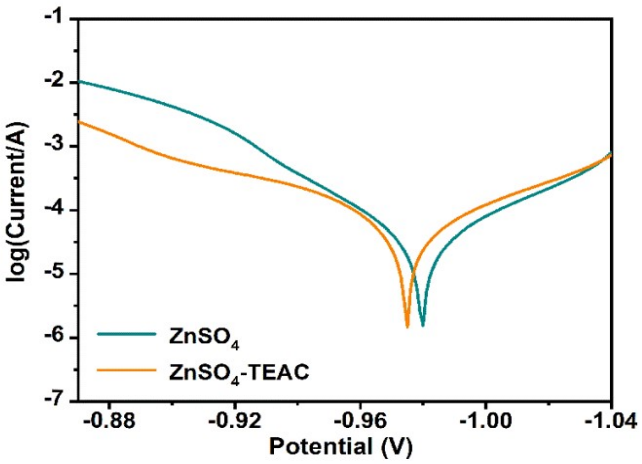

Figure S10. Tafel curves of Zn symmetric cell in the electrolyte without/with TEAC additive.

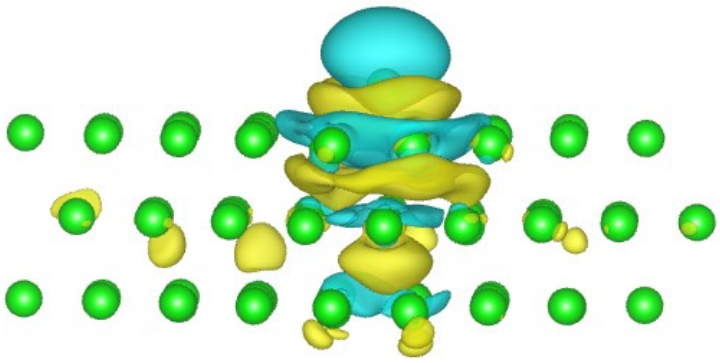

Figure S11. Differential charge density of Zn^{2+} on a Zn surface. The zinc ion, hydrogen, zinc atoms are marked as blue, yellow and green, respectively.

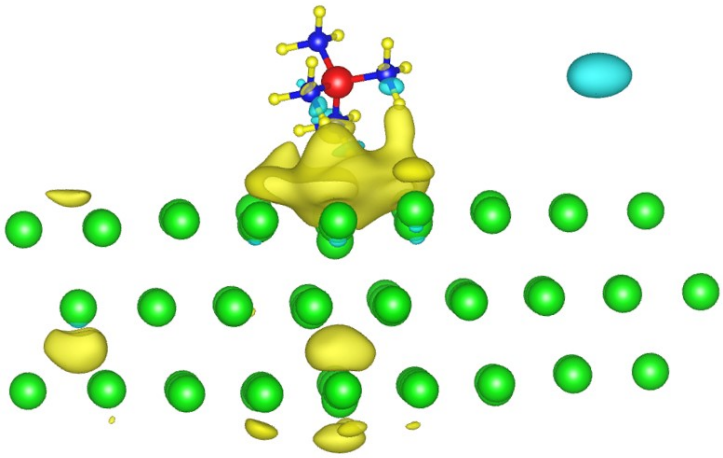

Figure S12. Differential charge density of TMA^+ on a Zn surface. The zinc ion, hydrogen, zinc, carbon and nitrogen atoms are marked as blue, yellow, green, purple and red, respectively.

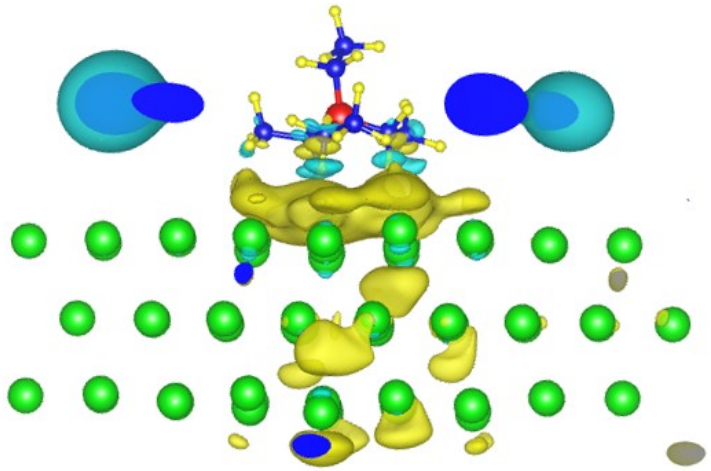

Figure S13. Differential charge density of TEA^+ on a Zn surface. The zinc ion, hydrogen, zinc, carbon and nitrogen atoms are marked as blue, yellow, green, purple and red, respectively.

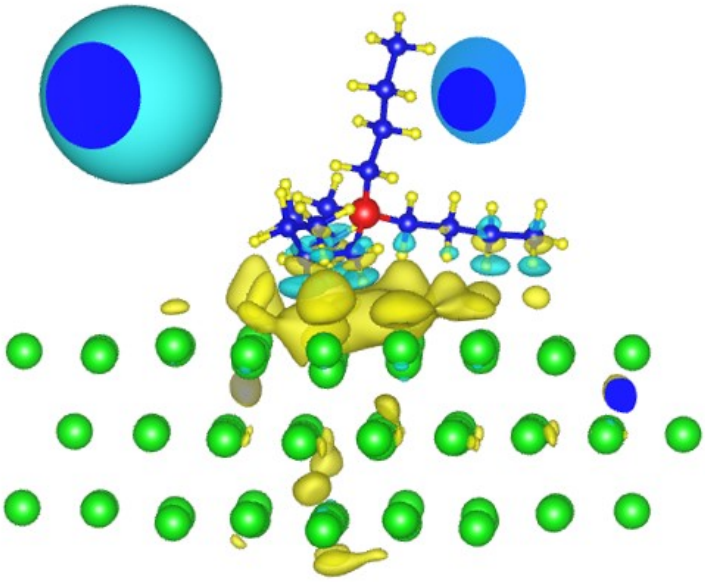

Figure S14. Differential charge density of TBA^+ on a Zn surface. The zinc ion, hydrogen, zinc, carbon and nitrogen atoms are marked as blue, yellow, green, purple and red, respectively.

References

S1 W. Wolfram, M. Rudolph and P. Brooker, Raman spectroscopy of aqueous $ZnSO_4$ solutions under hydrothermal conditions: solubility, hydrolysis, and sulfate ion pairing. *J. Solution Chem.*, 1999, **28**, 621–630.

S2 M. Rahman and J. Podder, Enhanced metastable zone width and optical properties of KCl doped $ZnSO_4 \cdot 7H_2O$ crystal grown by isothermal evaporation technique. *Bangladesh J. Sci. Res*., 2020, **2**, 88–95.

S3 M. Sawicka, P. Storoniak, J. B a ejowski and J. Rak, TG-FTIR, DSC, and quantum-chemical studies on the thermal decomposition of quaternary ethylammonium halides. *J. Phys. Chem. A*, 2006, **110**, 5066–5074.

S4 Y. Zhu, J. Yin, X. Zheng, A. Emwas, Y. Lei, O. Mohammed, Y. Cui and H. Alshareef, Concentrated dual-cation electrolyte strategy for aqueous zinc-ion batteries. *Energy & Environ. Sci.*, 2021, **14**, 4463–4473.